ELSEVIER

Journal of Nuclear Materials 290–293 (2001) 162–165

journal of nuclear materials

www.elsevier.nl/locate/jnucmat

Implantation, erosion, and retention of tungsten in carbon

R.A. Zuhr [b], J. Roth [a,*], W. Eckstein [a], U. von Toussaint [a], J. Luthin [a]

[a] *Max-Planck-Institut für Plasmaphysik, Boltzmannstr. 2, D-85748 Garching, Germany*
[b] *Oak Ridge National Laboratory, Oak Ridge, TN 37831, USA*

Abstract

The bombardment of C with 100 keV W at normal incidence is studied as a function of the incident W fluence experimentally and by computer simulation with the program TRIDYN. Calculated oscillations in the amount of retained W and in the target weight change are confirmed experimentally.

Keywords: Implantation; Erosion; Retention; Tungsten; Carbon

1. Introduction

In a future large fusion machine, ITER [1], three elements have been proposed to serve as first wall materials in different locations, Be for the main vessel wall, and C and W in the divertor. As shown earlier [2], in the case of bombardment of W with C, erosion will occur at large angles of incidence, whereas deposition prevails at normal incidence and small angles of incidence. Recently it has been found, that even oscillations in the sputtering yield as a function of fluence can occur [3]. Due to the strong implications of these kinds of effects in fusion plasma machines, it is the aim of this paper to show that these oscillation effects can also be observed experimentally.

2. Experimental procedure

The substrates used in this work were $12 \times 15 \times 0.5$ mm^3 rectangles of oriented high purity pyrolytic graphite supplied by Union Carbide, that were cut with the graphite planes either parallel or perpendicular to the sample surface. The blanks were mechanically polished to produce a mirror finish on the active surface.

Bombardment with 100 keV W ions was carried out on an Extrion model 200–1000 ion implantation accelerator at room temperature (sample holder held at 0°C). Temperatures were monitored by chromel-alumel thermocouples mounted in the sample holder. The vacuum in the chamber was typically in the low 10^{-7} mbar range during operation. The beam was rastered over a 20 mm diameter circular collimator in the x and y directions so that the beam was reduced from its unrastered value by approximately 30% in each direction to give reasonable uniformity over the implanted region. The question of beam uniformity will be addressed in greater detail in the discussion section.

The samples were weighed before and after each implantation using a Mettler microbalance with a sensitivity of 1 μg. The balance was zeroed before and after each measurement, but a drift could not be totally eliminated and the error in the measured masses was estimated to be ±3 μg. The amount of W retained in the samples was measured quantitatively after each dose using Rutherford backscattering spectrometry (RBS) with 2.3 MeV ^{4}He ions at a detector angle of 160° and with the sample tilted at 60° to the incident beam in the direction of the detector to improve the depth resolution. The RBS was done on a 1.7 MeV General Ionics Tandetron. Accurate depth profiles were extracted from the raw data using Bayesian statistics.

* Corresponding author. Tel.: +49-89 3299 1387; fax: +49-89 3299 2279.
E-mail address: roth@ipp.mpg.de (J. Roth).

0022-3115/01/$ - see front matter
PII: S0022-3115(00)00569-9

3. Evaluation of measured RBS-data

The small depth profile changes require a proper deconvolution of the apparatus function, which enhances the achievable resolution. The Bayesian probability theory provides a reliable way to solve this ill-posed linear inverse problem [4,6,8]. The measured edges of Au- and Si-samples have been used to determine the apparatus functions for each measured carbon-tungsten profile. The nonlinear inverse problem of depth profile determination from RBS data has been solved using the adaptive kernel concept combined with a forward simulation program for RBS spectra. In this simulation program, the sample is divided into layers with a linear concentration profile in each layer. Therefore, discontinous depth profiles are avoided. The necessary depth resolution is data-dependent calculated. The mathematical and numerical details of this approach are explained in [5,7]. The prior knowledge entering the calculation is, besides the restriction for the individual concentrations to be positive and to be summed up to unity in each layer, that there is no tungsten below a depth of 1×10^{19} atoms/cm^2. The main source of uncertainty in the results is the sensitivity of the depth profiles to the energy calibration, which therefore, requires special care.

4. Simulation

The Monte Carlo program TRIDYN [9,10] is used for the calculations. It is based on the static Monte Carlo program TRIM.SP [10,11], but takes dynamic target changes into account. A randomized target structure is assumed, and the atomic interactions are treated as a sequence of binary collisions. In all calculations the WHB (Kr–C) potential [12] is applied. The inelastic energy loss is described by an equipartition of the continuous Lindhard–Scharff [13] and the local Oen–Robinson [14] models.

A pseudo-projectile corresponds to an incoming fluence. After the collision cascade of each pseudo-projectile is finished, the target composition and density are updated by the reciprocal addition of the atomic densities of the pure elements according to the composition. The surface binding energy is chosen according to the surface composition as given in model 3 [15], where the surface binding energy is linearly interpolated between the corresponding values of the pure elements and the mean value of both species. TRIDYN allows the determination of sputtering yields, reflection coefficients, composition, depth profiles of the implanted species, and related values as a function of the incident fluence. The target weight changes according to the difference of the implanted amount and the amount removed from the target. The TRIDYN version used is adjusted for parallel computing [16] using eight processors on a CRAY-T3E.

Calculations have been performed for the bombardment of C with W at normal incidence for several incident energies. Diffusion and segregation are not taken into account.

5. Results and discussion

Implantation profiles of 100 keV W into C as calculated using TRIDYN are shown as a function of the implantation fluence in Fig. 1(b). As the calculated profiles do not include any post-implantational diffusion effects, they are best compared to experimental room temperature profiles, see Fig. 1(a).

Both experimental and calculated profiles show good agreement at the lowest fluences for the implantation profile of W into the pure carbon substrate. The mean range is about 40 nm, the width of the distribution at 10 nm is much smaller than the mean range. This is

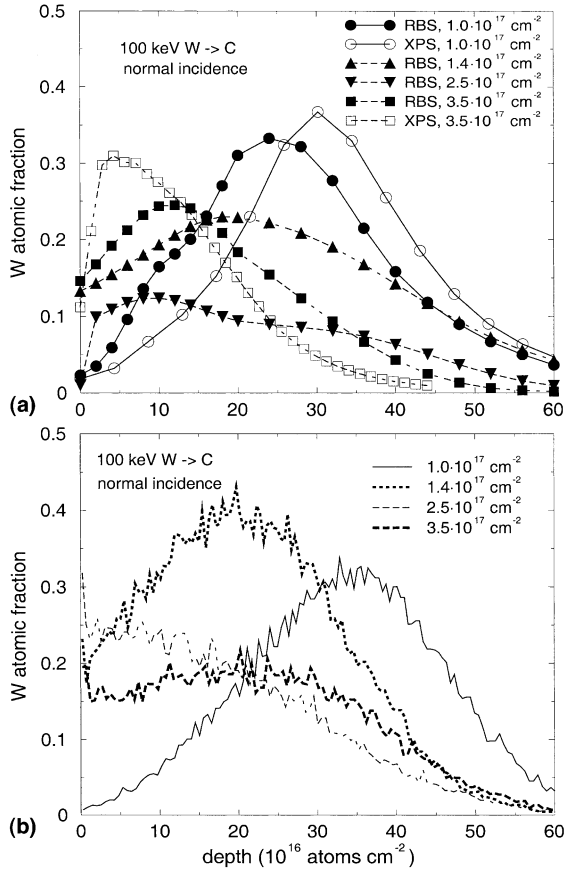

Fig. 1. W depth profiles at different fluences for the bombardment of C with 100 keV W at normal incidence: (a) experiment, (b) calculated with TRIDYN.

typical for heavy ion implantation into low-Z substrates, as the heavy ions cannot be scattered by angles larger than $\arcsin(M_2/M_1)$. With increasing fluence carbon surface atoms are sputtered, bringing previously implanted W atoms closer to the surface. In the present case the carbon sputtering yield, Y_C, due to 100 keV W ions is of the order of 2. A fluence of 4×10^{16} W atoms/cm^2 erodes two standard deviations and one half of the mean range. With continuous sputtering the resulting W profile flattens and the maximum concentration in the bulk gets close to $1/Y_C$, i.e., around 20 at.%.

At a fluence of 1×10^{17} atoms/cm^2, the erosion has brought the distribution so close to the surface that the W surface concentration increases. In addition to carbon sputtering, W sputtering also has to be considered. As the self-sputtering yield of W, Y_W, is about 3, the same amount of W is eroded as implanted at a surface concentration of $1/Y_W$, i.e., at 33 at.%. In order to reach steady state conditions, preferential sputtering of carbon atoms will increase the W concentration within the first monolayers to 33%, while in the bulk a flat W concentration of about 20% reaches to depths equivalent to the mean ion range. These features are clearly seen in the calculated steady state W profiles, while the increase at the surface is too narrow to be resolved in the experimental profiles.

These zero-order processes alone would lead to a continuous increase of the implanted amount of W with fluence until steady state is reached. However, two additional effects complicate the implantation process: a bulk W concentration of 20 at.% considerably enhances the nuclear and electronic stopping and scattering of incident ions reducing the mean ion range. The reduced ion range overlaps with the shifted implantation profile due to sputtering, resulting in high concentration of W. This over-saturation of W leads transiently to an implanted amount much larger than in saturation. As soon as this high W concentration reaches the surface, self-sputtering will rapidly reduce the W amount until a surface concentration of 33% is reached. At this stage, the narrow W profile contains fewer W atoms than reached in steady state. During further implantation, the profile broadens due to the lower electronic stopping and the steady state W concentration is reached after several successively smaller oscillations. The calculated and measured dependence of the implanted W amount with fluence at room temperature are compared in Fig. 2(a) and show excellent agreement. Another quantity which gives information about the erosion of the carbon substrate is the weight change of the probe. As W atoms are about 15 times heavier than carbon atoms, the probe will initially gain weight in oscillations similar to the implanted amount of W. Once steady state is reached, i.e., the implanted W amount stays constant, the following weight loss is a measure of the carbon sputtering yield (Fig. 2(b)). From the weight decrease with fluence a sputtering yield of 3.5 is de-

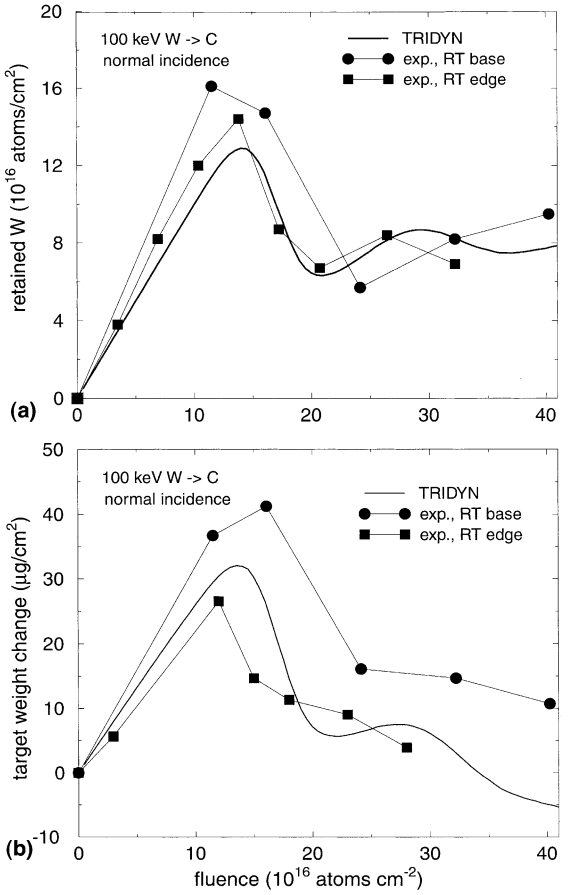

Fig. 2. 100 keV W implantation into C at normal incidence versus the incident W fluence: (a) retained W at room temperature and elevated temperatures; (b) target weight change at room temperature.

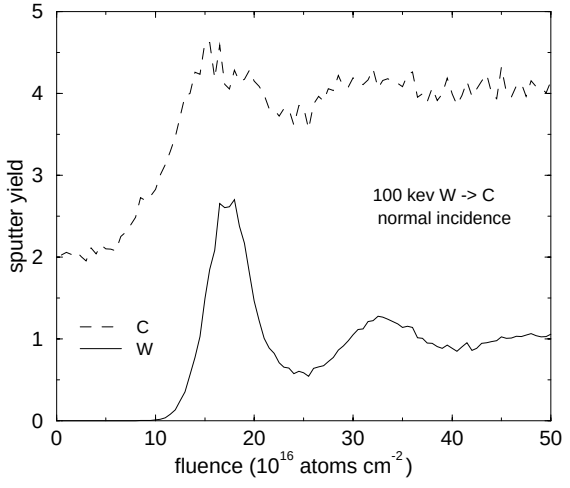

Fig. 3. Calculated partial sputtering yields of C and W versus the incident W fluence due to the bombardment of C with 100 keV W at normal incidence.

duced, which is in good agreement considering a surface concentration of carbon of only 67%. Fig. 3 shows the fluence dependence of the calculated sputtering yields for C and W.

6. Conclusion

W implantation profiles in carbon, the retained amount of W, and carbon erosion at room temperature can well be reproduced by dynamic implantation codes such as TRIDYN. As the self-sputtering of W above an energy of 1 keV is larger than unity, at high fluences a saturation in the implanted amount is reached. The oscillatory behavior in approaching this steady state is due to changes in the implantation profile and carbon surface erosion.

Acknowledgements

Research sponsored by the US Department of Energy under contract DE-AC05-00OR22725 with the Oak Ridge National Laboratory, managed by UT-Batelle, LLC.

References

[1] ITER Physics Expert Group on Divertor, ITER Physics Expert Group on Divertor Modelling and Database, ITER Physics Basis Editors, ITER EDA, Nucl. Fus. 39 (12) (1999) 2391 (Chapter 4).
[2] W. Eckstein, J. Roth, Nucl. Instrum. and Meth. B 53 (1991) 279.
[3] W. Eckstein, Nucl. Instrum. and Meth. B 171 (2000) 435.
[4] R. Fischer, M. Mayer, W. von der Linden, V. Dose, Nucl. Instrum. and Meth. B 136–138 (1998) 1140.
[5] R. Fischer, M. Mayer, W. von der Linden, V. Dose, Phys. Rev. E 55 (1997) 6667.
[6] V. Dose, R. Fischer, W. von der Linden, in: G. Erickson (Ed.), Maximum Entropy and Bayesian Methods, 1998, pp. 147–152.
[7] U. von Toussaint, K. Krieger, R. Fischer, V. Dose, New J. Phys. 1 (1999) 11.
[8] W. von der Linden, Appl. Phys. A 60 (1995) 155.
[9] W. Moeller, W. Eckstein, J.P. Biersack, Comp. Phys. Commun. 51 (1988) 355.
[10] W. Eckstein, Computer Simulation of Ion-Solid Interaction, Springer Series in Materials Science, Vol. 10, Springer, Berlin, Heidelberg, 1991.
[11] J.P. Biersack, W. Eckstein, Appl. Phys. A 34 (1984) 73.
[12] W.D. Wilson, L.G. Haggmark, J.P. Biersack, Phys. Rev. B 15 (1977) 2458.
[13] J. Lindhard, M. Scharff, Phys. Rev. 124 (1961) 128.
[14] O.S. Oen, M.T. Robinson, Nucl. Instrum. and Meth. 132 (1976) 647.
[15] W. Eckstein, M. Hou, V.I. Shulga, Nucl. Instrum. and Meth. B 119 (1996) 477.
[16] W. Eckstein, R. Dohmen, H. Friedrich, F. Hertweck, Nucl. Instrum. and Meth. B 153 (1999) 345.